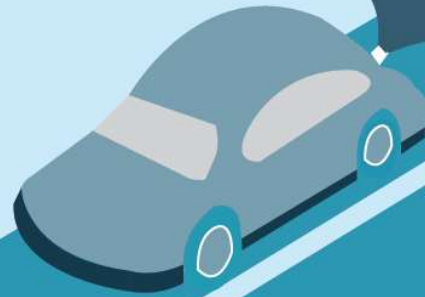


# Mobile-Monitoring Campaign for Air-Pollution Studies in Bengaluru





# Mobile-Monitoring Campaign for Air-Pollution Studies in Bengaluru

**Center for Study of Science, Technology and Policy (CSTEP)**

**ILK Labs**

October 2020

Center for Study of Science, Technology and Policy (CSTEP) is a private, not-for-profit (Section 25) Research Corporation registered in 2005.

ILK Labs (registered as ILK Consultancy LLP) is a research and educational organisation, established in May 2017 with a goal to design and implement educational and research programmes in environment and sustainability.

Designed and edited by CSTEP

#### Disclaimer

While every effort has been made for the correctness of data/information used in this report, neither the authors nor CSTEP accepts any legal liability for the accuracy or inferences for the material contained in this working series and for any consequences arising from the use of this material.

© 2020 Center for Study of Science, Technology and Policy (CSTEP)

Any reproduction in full or part of this publication must mention the title and/or citation, which is provided below. Due credit must be provided regarding the copyright owners of this product.

Contributors: Dr Sreekanth Vakacherla (CSTEP); Meenakshi Kushwaha (ILK Labs)

*(The author list provided assumes no particular order as every individual contributed to the successful execution of the project.)*

This working series should be cited as: CSTEP & ILK Labs (2020). Mobile-monitoring campaign for air-pollution studies in Bengaluru. (CSTEP-WS-2020-04).

October, 2020

#### Center for Study of Science, Technology and Policy

#### ILK Labs

##### Bengaluru Office

18-19, 10<sup>th</sup> Cross, Mayura Street  
Papanna Layout, Nagashettyhalli, RMV II Stage

62/H, 1<sup>st</sup> Floor, Modi Residency  
Millers Road, Benson Town

Bengaluru-560094, Karnataka (India)  
Tel.: +91 (80) 6690-2500

Bengaluru-560046  
Karnataka (India)  
Tel.: +91 (80) 4371-7396

##### Noida Office

1<sup>st</sup> Floor, Tower A  
Smartworks Corporate Park  
Sector 125, Noida-201 303

Uttar Pradesh (India)

**Email:** [cpe@cstep.in](mailto:cpe@cstep.in)

**Website:** [www.cstep.in](http://www.cstep.in)

## Acknowledgements

We would like to take this opportunity to thank our funders, collaborators, and colleagues for their continued support and guidance throughout the project.

First of all, we thank MacArthur Foundation for providing financial support to CSTEP for conducting air-pollution studies in Bengaluru.

We would like to thank Prof. Julian Marshall, University of Washington (UW), for conceiving the idea of mobile-monitoring in Bengaluru back in 2018. We express sincere gratitude to Prof. Joshua Apte, University of Texas—Austin (UT), for his expert advice and help in adapting the mobile-monitoring approaches and lessons learnt in California to the project in Bengaluru. We also acknowledge Jonathan Gingrich (UT) for brainstorming and helping set up the mobile platform.

We convey our sincere gratitude to Adithi Upadhy and Pratyush Agarwal for their critical role in data collection and analysis at ILK, and to Elbin Savio at ILK for providing logistical support on all aspects of the project.

Our sincere thanks are due to Saptak Ghosh and Nikhilesh Dharmala (internal reviewers) and Dr Vijay Kanawade, Centre for Earth, Ocean and Atmospheric Sciences, University of Hyderabad, Hyderabad (external reviewer), for their critical inputs on the project.

We also take this opportunity to acknowledge the CSTEP project leadership—Dr Jai Asundi, Dr Pratima Singh, and Priyavrat Bhati—for their valuable support and guidance throughout, as well as a special mention to Dr Bellarmine for programmatic support. We could not have completed this project without Ashwath (CSTEP Driver), who patiently drove on small streets and highways for the data collection, and E. Manjunatha (Manager—Purchase, Facilities and Administration).

Finally, we thank the Central Pollution Control Board (CPCB) and Karnataka State Pollution Control Board (KSPCB) for installing and maintaining the continuous ambient air-quality monitoring stations and making the data publicly available.

## Abbreviations and Acronyms

Abbreviations	Expansions
ANOVA	Analysis of Variances
ATN	Attenuation
BAM	Beta-Attenuation Monitor
BBMP	Bruhat Bengaluru Mahanagara Palike
BC	Black Carbon
CBD	Central Business District
cm	Centimetre
CNG	Compressed Natural Gas
CPC	Condensation Particle Counter
CPCB	Central Pollution Control Board
CSTEP	Center for Study of Science, Technology and Policy
CV	Coefficient of Variation
DR	Dilution Ratio
GPS	Global Positioning System
HEI	Health Effects Institute
IQR	Inter-Quartile Range
IST	Indian Standard Time
KAN	Kannuru
KSPCB	Karnataka State Pollution Control Board
km	Kilometre
kmph	Kilometres per hour
LMIC	Low- and Middle-Income Countries
LPM	Litres Per Minute
MAL	Malleswaram
mLPM	Millilitres Per Minute
mg	Milligram
nm	Nanometre
NAAQS	National Ambient Air Quality Standards
NCAP	National Clean Air Programme
ORR	Outer Ring Road

OSM	Open Street Map
PCB	Pollution Control Board
PM <sub>10</sub>	Particulate matter 10 micrometres or less in diameter
PM <sub>2.5</sub>	Particulate matter 2.5 micrometres or less in diameter
RH	Relative humidity
SD	Standard deviation
Tr	Transmission
UFPs	Ultrafine particles
UPS	Uninterrupted Power Supply
URT	Urban-Rural Transect
WHO	World Health Organization

## Executive Summary

Stationary air-quality monitoring is a common component of understanding air-pollution; however, monitoring at one location fails to capture local variations in pollutant concentrations. In locations where emissions and concentrations exhibit fine-scale spatial variability, including in urban environments in India, characterising spatial variability can be helpful for understanding sources and potential solutions for air-pollution. 'Mobile monitors', that is, sensors installed on a mobile platform, have been used as a new approach across the world, by cities and governments to complement their existing stationary monitoring networks.

This report summarises the outputs of an 11-month-long mobile-monitoring project with a goal to produce a high-resolution pollution map of select parts of Bengaluru. The aim of this project was also to study the contrast in urban areas and examine if these contrasts are reflected in measured pollutant concentrations. The data thus collected will help in building and validating predictive models in the future. A custom-built mobile platform, comprising a CNG car equipped with air-pollution instrumentation, was used in the study. Our route of study included a central business district (CBD), a residential urban neighbourhood, a peri-urban neighbourhood, and an urban-rural transect. In the entire project, the study route was surveyed about 27 times (~6000 km of driving).

During the study period, nearly a million 1-second measurements of each of the pollutants were made. Overall, large spatial gradients were observed in on-road pollutant concentrations. Major roads had the highest pollutant levels, followed by arterials and residential roads. Among individual pollutants, black carbon (BC) and ultrafine particles (UFPs) were characterised with large spatio-temporal variations, compared with that of PM<sub>2.5</sub> (a criteria pollutant).

The on-road BC and PM<sub>2.5</sub> are several times higher than ambient levels. Additionally, PM<sub>2.5</sub> over the major roads is always higher than the prescribed national standards. Not surprisingly, the urban residential neighbourhood was characterised by relatively low levels of on-road pollution (PM<sub>2.5</sub> values were the lowest there). Similarly, BC and UFPs were the lowest in residential neighbourhoods (urban and peri-urban), followed by arterials and major roads. All of the measured pollutants peaked at different locations along the study route. While UFPs peaked in the central business district characterised by commercial activity, BC and PM<sub>2.5</sub> peaked away from the city centre, along major roads.

The study investigated the feasibility of mobile-monitoring studies in middle-income countries, which often have poor road conditions (making such measurement campaigns challenging), high background pollution levels, and heterogeneous sources of pollution. This project has demonstrated that this approach is feasible and leads to reliable estimates of street-level exposure. This approach can be tailored to study specific sources or regions and zoom in to identify hotspots that may be prioritised for policy interventions. The next steps would be to scale this approach in a way that best suits the needs of local policymakers.



## Contents

1. Introduction .....	13
1.1. Need for Mobile-Monitoring .....	14
1.2. Aim and Objectives .....	14
1.3. Scope and Limitations .....	15
1.3.1. Data Noise .....	15
1.3.2. Choice of Vehicle .....	15
1.3.3. Labour-Intensive / Manual Navigation .....	15
2. Materials and Methods .....	17
2.1. Instrumentation .....	17
2.1.1. PM <sub>2.5</sub> Measurements .....	17
2.1.2. Black Carbon (BC) Measurements .....	17
2.1.3. Ultrafine Particles (UFPs) Measurements .....	18
2.1.4. Global Positioning System (GPS) .....	19
2.1.5. Mobile Platform .....	19
2.2. Data Correction .....	20
2.2.1. PM <sub>2.5</sub> .....	20
2.2.2. Black Carbon (BC) .....	20
2.2.3. Ultrafine Particles (UFPs) .....	21
2.2.4. Hour-of-the-day Correction .....	21
2.3. Snapping and Gridding .....	21
2.4. Study Route .....	22
2.5. Study Period .....	23
3. Results .....	25
3.1. Number of Measurement Points .....	25
3.2. Choice of Central Tendencies .....	25
3.3. Spatial Variations .....	27
3.4. Stability Analysis .....	31
3.5. Comparison with Ambient Data .....	32
3.6. Spatial Gradient and Hotspot Areas .....	34
4. Conclusions and Way forward .....	37
5. References .....	39
6. Appendix .....	41



## Figures

Figure 1 DustTrak aerosol monitor (model: 8530) .....	17
Figure 2 microAeth (model: AE51) .....	18
Figure 3 Handheld Condensation Particle Counter (model: 3007) .....	18
Figure 4 Garmin GPSMAP-64s .....	19
Figure 5 Instrument crate and laptop in the retrofitted rear shelves .....	20
Figure 6 Study route; MAL (green), CBD (yellow), KAN (blue), urban-rural transect (red). The OSM background grey lines indicate roads, while grey patches indicate water bodies and green areas.....	22
Figure 7 Number of (1-second) measurements made in each 30-m road segment within the study period for a) PM <sub>2.5</sub> , b) BC, and c) UFPs.....	26
Figure 8 Spatial maps of various pollutants.....	28
Figure 9 Zoomed-in spatial maps for MAL.....	29
Figure 10 Distribution of pollutants as per road classification. A steeper gradient is seen in BC compared with the others. In the box plot, the solid dot represents the mean, central line of the box represents the median, and the box represent the 25 and 75 percentiles, whiskers represent the 5 and 95 percentile values of the distribution.....	30
Figure 11 Monte-Carlo sub-sampling analysis for PM <sub>2.5</sub> , BC and UFPs.....	31
Figure 12 Comparison of (1-second) on-road and ambient PM <sub>2.5</sub> . In the box-plot, solid dot represents the mean, central line of the box represents the median, and the box represent the 25 and 75 percentiles, whiskers represent the 5 and 95 percentile values of the distribution.....	32
Figure 13 Comparison of on-road and (CSTEP) ambient BC .....	33
Figure 14 Spatial gradients in PM <sub>2.5</sub> , BC and UFPs. The red line represents the fitter polynomial, and the shaded part represents the 95% confidence interval (CI). Only the major roads were considered to plot the gradients. ....	35
Figure 15 Relationship between DustTrak PM <sub>2.5</sub> and BAM PM <sub>2.5</sub> . Solid blue line indicates the linear least square fit. Dotted line indicates the 1:1 line.....	41
Figure 16 (top panel) Raw PM <sub>2.5</sub> from DustTrak; (bottom panel) BAM corrected DustTrak PM <sub>2.5</sub> .....	42
Figure 17 (top panel) Raw BC from AE51; (middle panel) spurious points removed BC; (bottom panel) spurious points removed and loading corrected BC .....	43
Figure 18 (top panel) Monthly hour-of-the-day correction factors for PM <sub>2.5</sub> , and (bottom panel) BC.....	44
Figure 19 (top panel) Raw GPS measurements; (middle panel) snapped GPS measurements; (bottom panel) gridded road segments. ....	45
Figure 20 Comparison between various central tendencies (for UFPs). Solid blue line indicates the linear least square fit. Dotted line indicates the 1:1 line. R-square values and the regression coefficients are given in the respective panels.....	46
Figure 21 Road classification based on OSM road features. Major roads, arterials, and residential roads consist of 2,895, 1,112 and 983 30-m road segments respectively .....	47

## Tables

Table 1 Pollutant statistics as per road classification .....	30
Table 2 Monthly mean on-road and ambient PM <sub>2.5</sub> (from various measurement sites, in $\mu\text{g m}^{-3}$ ) .....	33
Table 3 Monthly mean on-road and ambient BC (in $\mu\text{g m}^{-3}$ ) .....	34

## 1. Introduction

Evidence of the harmful effects of air-pollution has been accumulating from the 1950s, back when the London Smog killed over 10,000 people. Since then, air-pollution has been known to affect almost every major organ system, including cardiovascular, respiratory, and neurology (Kim et al., 2015; Schraufnagel et al., 2019).

Most of the studies that enhance our understanding of health impacts of air-pollution come from developed countries with relatively cleaner air. Comparatively few studies were conducted in countries where the air is the dirtiest. Such studies are important because health effects do not necessarily follow a linear pattern and results from regions with much lower pollution levels may not be readily translated to highly polluted low- and middle-income countries (LMICs) (Tonne 2017). Additionally, LMICs' pollution sources (e.g., coal power plants, diesel vehicles, domestic heating and lighting, garbage and agricultural burning) are different from those in developed countries, and exposure from these sources and their toxicological impacts remain less well characterised.

PM<sub>2.5</sub>, (mass concentration of particulate matter with diameter less than or equal to 2.5 micrometres (µm)), because of its small size, can enter and lodge deep in our lungs and can even enter the bloodstream. Chronic exposure to PM<sub>2.5</sub> contributes to a risk of cardiovascular and respiratory diseases. In 2016, long-term exposure to PM<sub>2.5</sub> caused more than an estimated 1.2 million deaths in India (Polk 2019). Black carbon (BC, a component of particulate matter) is an indicator of combustion-related pollution sources; its major sources are combustion engines (mainly diesel), coal-based power plants, biomass cooking, and agricultural waste burning. The health outcomes associated with PM<sub>2.5</sub> are also associated with BC (Janssen et al., 2011). Latest evidence shows that ambient BC can enter the foetal side of the placenta, leading to direct exposure to the developing foetus (Bongaerts et al., 2019). Another important metric of particulate-matter-air-pollution is ultrafine particle number concentration (UFPs, particles with size less than 100 nanometres (nm)). UFPs are either emitted directly from a source or formed by precursor gases. These particles have not been studied as extensively for their health effects as PM<sub>2.5</sub>, but evidence regarding their detrimental health effects is beginning to accumulate (Ohlwein et al., 2019). Given their size, UFPs, upon entering the lungs, can move to many organs of the body. Short-term exposure to UFPs is associated with increased blood pressure and pulmonary inflammation, thus elevating the risk of cardiovascular disease.

Pollution exposure and its health effects depend on concentrations in different microenvironments that people spend time in. Traffic-related emissions are known to influence ambient air-quality and personal exposures with an exposure zone of up to 500 metres (m) from roadways (source regions of these emissions) (HEI, 2010). However, traffic as an exposure micro-environment has been sparsely studied in India. In a first-of-its-kind study in Delhi, Apte et al., (2011) revealed that, with an average PM<sub>2.5</sub> of around 90 µg m<sup>-3</sup> (1.5 times the Indian National Ambient Air Quality Standard (NAAQS) for daily mean PM<sub>2.5</sub>) and BC at around 42 µg m<sup>-3</sup>, personal exposure during a short-term auto rickshaw commute alone is comparable to the daily exposure of individuals in a high-income country. Furthermore, an assessment of on-road exposure in different commute modes in Delhi revealed that traveling in an auto rickshaw leads to 30% more exposure than an off-road location because of the proximity to on-road traffic sources. Among various commute modes, cycling led to the maximum exposure, when

compared with other transport modes including bus, car, walking, and metro (Goel et al., 2015). Notably, no such studies have been conducted in other Indian cities until now. In Bengaluru, Dekoninck et al., (2015) developed a model for in-traffic exposure of bi-cyclists to BC and UFPs based on spectral evaluation of mobile noise measurements.

### 1.1. Need for Mobile-Monitoring

Fixed-site monitoring generally does not capture local variations in air-pollution. Previous studies employing sensors-on-a-car or mobile-monitoring approach in Oakland, California, have demonstrated that air-pollution can vary up to eight times within a city block (Apte et al., 2017). This is especially true for Indian cities, where sources are more heterogeneous than those in the developed world. To develop a better understanding of the actual exposure of residents and variation in levels of air pollutants from street to street, mobile-monitoring is a fitting approach to provide a highly contextual and hyper-local understanding of air-pollution in a city.

Mobile-monitoring is also envisaged to be a diagnostic tool to develop evidence-based actions towards air-pollution mitigation measures at a city, community, and individual level. It is expected to act as a powerful supplement to the fixed-site regulatory network, bridging the gaps that currently exist. From a parallel-monitoring-systems point of view, mobile-monitoring is essentially thought to reside between fixed and personal monitoring, where it might not provide air-pollution measurement for each individual's personal environment, but can come closest to locations where people live, work, commute, and generally spend their time.

While the mobile-monitoring approach is gaining popularity, both for research studies and government monitoring programmes, in developed nations (e.g., Breathe London, 2018), studies in India have been limited. In the Delhi study cited earlier, Apte et al., (2011) collected around 180 hours of on-road measurements of BC, PM<sub>2.5</sub>, and UFPs over 37 km of road length. This study confirmed that on-road exposures in Indian settings are much higher than stationary ambient measurements, and reinforced the understanding that ambient monitoring does not capture the true exposure. In another study, researchers measured personal exposure on nearly 200 km of highway length in different commute modes and concluded that PM<sub>2.5</sub> exposure was the highest in an open car, followed by that in a bus and it was the lowest in an air-conditioned car (Kolluru et al., 2018). So far, no such exhaustive study has been conducted in Bengaluru, which could have contributed to a better understanding of on-road pollution levels within the city.

### 1.2. Aim and Objectives

The aim of the current project was to study the contrast in urban areas and examine whether these contrasts are reflected in the measured pollution levels. Towards this goal, we measured on-road particulate matter (BC, PM<sub>2.5</sub>, and UFPs) using a mobile platform.

We achieved the following specific objectives via this study:

- Exploring the potential of mobile-monitoring in Indian urban and peri-urban settings
- Studying spatial gradients in on-road air-pollution
- Identifying hotspots along the study route
- Developing high-resolution pollution maps of the study regions

### 1.3. Scope and Limitations

This study examined air-quality in various neighbourhoods and some major roads of Bengaluru, via mobile-monitoring. Approximately, 27 complete route measurements (spanning over 150 unique kilometres (km)) were made. The results may also be applicable to other regions of Bengaluru and other Indian metropolitan cities with similar urban settings as of the areas sampled in this study. The measurements were limited to weekday morning hours (9 am to 1 pm, local time). Some operational challenges that we experienced are listed below.

#### *1.3.1. Data Noise*

Air-pollution measurements (especially from optical instruments) on a mobile platform are susceptible to vibration-related noise because of the (poor) road conditions and vehicle-suspension effectiveness.

#### *1.3.2. Choice of Vehicle*

Our monitoring platform was a car fuelled by CNG (compressed natural gas), which is low-emitting but not completely emissions-free. The emissions from the vehicle can bias the measurements. An electric vehicle (i.e., a zero-emissions vehicle) would be the best choice for a mobile platform, but the battery capacity of the vehicle limits the number of monitoring kilometres per session.

#### *1.3.3. Labour-Intensive / Manual Navigation*

Our approach involved measurements on each and every road in a neighbourhood, including small lanes (which can be missed by automatic navigation). Factors like unplanned and indefinite road closures and poor road conditions led to occasional changes of the study routes, which necessitated manual navigation.





## 2. Materials and Methods

### 2.1. Instrumentation

All the instrumentation used for the mobile-monitoring campaign were portable, battery-operated, and capable of measuring and logging at high temporal resolution (1-second interval). All the instruments were factory calibrated, before the campaign. A logging interval of 1 second was chosen to maximise the number of data points within a given size of road segment. All instrument times were synchronised to GPS time on a regular basis.

#### 2.1.1. $PM_{2.5}$ Measurements

DustTrak II Aerosol Monitor (model: 8530, TSI, Shoreview, USA) was used to measure  $PM_{2.5}$  concentrations. DustTrak utilises the well-established aerosol light-scattering technique to estimate real-time aerosol mass loadings. It uses a sheath air system that isolates the aerosol in the optics chamber to keep the optics clean for improved reliability and low maintenance. DustTrak works at a flow rate of 3 LPM (litres per minute). Detailed specifications of the instrument can be found at <https://tsi.com/products/aerosol-and-dust-monitors/dust-monitors/dusttrak-ii-aerosol-monitor-8530/>.

During the campaign, DustTrak, fitted with a manufacturer-supplied 2.5-micron size selective (inertial) impactor, was operated at 1-second log interval to measure and record the real-time  $PM_{2.5}$ . As a part of regular maintenance, zero calibration was performed on a daily basis before the start of the measurement campaign.

$PM_{2.5}$  measured with the light-scattering technique is sensitive to the optical properties of the local aerosol mixture (which will be quite different from that used for the factory calibration of DustTraks), aerosol size distribution, and atmospheric humidity levels. All of these sensitivities of the DustTrak-measured  $PM_{2.5}$  were addressed by applying a relevant correction factor, the procedure for which is outlined in Section 2.2.



Figure 1 DustTrak aerosol monitor (model: 8530)

Source: [www.tsi.com](http://www.tsi.com)

#### 2.1.2. Black Carbon (BC) Measurements

A microAeth (model: AE51, AethLabs, San Francisco, USA) was used to measure BC mass concentrations. AE51 is a highly sensitive, palm-held, and battery-operated instrument designed for measuring the optically absorbing BC component of aerosol particles. It measures the rate of change in the absorption of transmitted light (880 nm) due to continuous collection of aerosol load on the filter ticket. During the monitoring, AE51 was set to operate at a flow rate

of 100 mLPM (millilitres per minute) and at a logging interval of 1-second. More details on AE51 can be found at <https://aethlabs.com/microaeth/ae51/overview>.

Because of AE51's sensitivity to instrument vibration and filter-loading effects, we applied data cleaning and loading-correction algorithm before using the data for further analysis. The correction algorithms are detailed in Section 2.2.



Figure 2 microAeth (model: AE51)

Source: [www.aethlabs.com](http://www.aethlabs.com)

### 2.1.3. Ultrafine Particles (UFPs) Measurements

An alcohol-based handheld Condensation Particle Counter (CPC, model: 3007, TSI, Shoreview, USA) was used to measure the ultrafine particle number concentrations. CPC works on the optical-detection principle and operates at a flow rate of 0.7 LPM. Aerosol particles present in the sample stream act as sites for the isopropyl alcohol to condense; particles grow into large alcohol droplets, which eventually get detected and counted in the optical chamber. The instrument detects and measures the particles in the size range of 10 nanometres to >1 micrometre. Detailed specifications of CPC3007 can be found at [https://tsi.com/products/particle-counters-and-detectors/condensation-particle-counters/condensation-particle-counter-\(cpc\)-3007/](https://tsi.com/products/particle-counters-and-detectors/condensation-particle-counters/condensation-particle-counter-(cpc)-3007/).

Owing to the measurement limitation of CPC3007 (measurement range: 0 to 1,00,000 particles per cubic centimetre ( $\text{cm}^{-3}$ )) and the general nature of very high urban particle number concentrations ( $> 100,000 \text{ cm}^{-3}$ ), the CPC was operated with a diluter (dilution ratio:  $\sim 5.5$ ). The description of the diluter is given in Ban-Weiss et al., (2009) and Apte et al., (2011) and not repeated here. Zero check of CPC3007 was performed before each measurement session to ensure proper operation of the instrument.



Figure 3 Handheld Condensation Particle Counter (model: 3007)

Source: [www.tsi.com](http://www.tsi.com)

### 2.1.4. Global Positioning System (GPS)

GPSMAP-64s (Garmin, USA) was used to register the GPS coordinates of the mobile-monitoring vehicle during the campaign. GPSMAP-64s works on the 'trilateration' mathematical principle of GPS and usually connects to 4 satellites to give the accurate location. More technical details of the instrument can be found at <https://support.garmin.com/support/manuals/searchManuals.faces?>



Figure 4 Garmin GPSMAP-64s

Source: [www.garmin.com](http://www.garmin.com)

### 2.1.5. Mobile Platform

The mobile platform was a CNG hatchback car (Maruti Suzuki Celerio). The instrument platform was custom-fit by replacing a part of the rear passenger seat with instrument shelves. The instruments operated on their own battery backup; there were no alternative arrangements (like UPS + battery system) for powering the instruments in the car. The air sample was drawn by individual instrument inlets, which were extended through the rear side window. The measuring equipment was cushioned using suitable materials to dampen the vibration during the rides. In the initial months of the project, a diesel car was used as the mobile platform. It was later replaced with a CNG car, to avoid possible contamination of the data collected by the instrument due to the monitoring vehicle's own tailpipe emissions. The data collected from the diesel and CNG cars was analysed for any possible bias, and the difference between the data collected from the two platforms was found to be within the limits of instrumental uncertainty.

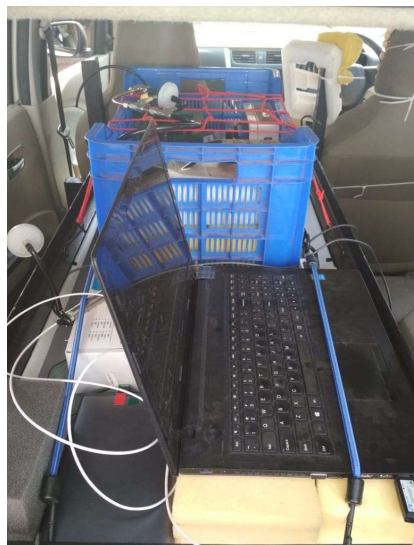


Figure 5 Instrument crate and laptop in the retrofitted rear shelves

## 2.2. Data Correction

Different instruments have various sensitivities and require cleaning and/or corrections to arrive at real values. In this section, various data correction and cleaning methodologies that were applied on the instrument-measured raw data are detailed.

### 2.2.1. $PM_{2.5}$

Due to the sensitivity of the optically measured  $PM_{2.5}$  (by DustTrak) to the local aerosol properties, DustTrak  $PM_{2.5}$  was compared with that of a Beta Attenuation Monitor (model: BAM1022, MetOne Instruments, GrantsPass, USA) in a collocation experiment conducted on the CSTEP terrace. BAM1022, which is equipped with a heating inlet and 2.5-micrometre sharp-cut cyclone, is a reference-grade instrument that measures  $PM_{2.5}$  based on the beta-attenuation principle. This experiment yielded a linear calibration (correction) equation (shown below), which was applied to the DustTrak-measured  $PM_{2.5}$ . We considered only day-time data to arrive at this equation.

$$[BAM\ PM_{2.5}] = 0.21 * [DustTrak\ PM_{2.5}] + 11.1 \quad (\text{equation 1})$$

The calibration plot and its application on a sample DustTrak  $PM_{2.5}$  dataset is shown in the Appendix.

### 2.2.2. Black Carbon (BC)

The sensitivity of AE51 to vibration (which is unavoidable in a moving platform) and shock results in frequent spurious spikes in the measured BC. The raw data from the instrument needs post-processing. We applied the post-processing algorithm developed and tested by Apte et al., (2011), on the raw measurements. This algorithm identified the spurious values in the raw measurements with respect to the baseline range of the instrument noise in the measured 1-second data. The algorithm flagged about 5% of the AE51-measured BC as spurious.

It is well established that filter-based real-time measurements underestimate BC concentrations as the filter loading of BC mass increases, which is termed as the 'loading effect'. Hence, we

applied the loading-correction equation developed by Ban-Weiss et al., (2009), on the cleaned (spurious spikes removed) BC measurements. The equation is shown below.

$$BC_{corr} = BC_{raw} * (0.88 * Tr + 0.12)^{-1} \quad (\text{equation 2})$$

$$Tr = \exp(-ATN/100) \quad (\text{equation 3})$$

$Tr$  is the filter transmission.  $BC_{raw}$  and  $ATN$  are the instrument-reported concentration and attenuation values.  $BC_{corr}$  is the loading-corrected BC.

The performance of the data-cleaning algorithm and loading correction is shown graphically in the Appendix.

### 2.2.3. Ultrafine Particles (UFPs)

A diluter, characterised by a dilution ratio (DR) of about 5.5, is used to dilute the sample flow of the CPC during mobile measurements. The raw particle count ( $UFPs_{raw}$ ) measured by the CPC with the diluter system needs to be multiplied with the  $DR$  to determine the real concentrations.

$$UFPs = UFPs_{raw} * DR \quad (\text{equation 4})$$

$UFPs$  represent the dilution-corrected particle number concentrations.

### 2.2.4. Hour-of-the-day Correction

The mobile-monitoring campaign lasted for four hours each day (from 9 am to 1 pm, local time). The choice of the measurement hours was governed by the battery backup of the different instruments. Within a day, urban ambient particulate pollution concentrations vary as a result of boundary-layer variations and dynamic emissions. The bias introduced by the diurnal variation in mobile-monitoring-measured  $PM_{2.5}$  and BC are corrected using a multiplication factor derived from the ambient measurements made by BAM1022 and a rack-mount aethalometer (model: AE33, Magee Scientific, Berkeley, USA) at CSTEP. This correction is termed as 'hour-of-the-day' correction and was detailed in Apte et al., (2017). We applied this correction on  $PM_{2.5}$  and BC, after getting them corrected for the instrument artefacts, as detailed previously. As ambient UFP measurements were not available, this correction was not applied on the mobile UFP measurements. The monthly mean 'hour-of-the-day' correction factors for  $PM_{2.5}$  and BC are shown in the Appendix. This correction procedure assumes that the diurnal variation is spatially invariant (note that the monitoring route consists of both urban and rural areas). On an average, this correction procedure enhanced  $PM_{2.5}$  and BC values by nearly 9% and 4% respectively.

In the rest of the document,  $PM_{2.5}$  represents BAM1022 and hour-of-the-day corrected DustTrak measurements in  $\mu\text{g m}^{-3}$  (microgram per cubic metre). BC represents cleaned, loading and hour-of-the-day corrected AE51 measurements in  $\mu\text{g m}^{-3}$ . UFPs represent dilution-factor-adjusted CPC measurements in  $\text{cm}^{-3}$ .

## 2.3. Snapping and Gridding

GPS measurements generally have an offset of 3–5 metres. Snapping is a technique used to map-match the GPS-measured location. A 'k-nearest neighbour' algorithm is used for assigning the noisy GPS measurements to the nearest Open Street Map (OSM) road feature.

For gridding, the road lengths are divided into 30-m road segments. The median and mean of the 1-second measured pollutant concentrations falling within each road segment was considered as the representative value for that particular road segment. We prepared 30-m gridded median and mean maps for the study route on a daily basis for all the pollutants. An illustration of raw and snapped GPS points and gridded road segments are shown in the Appendix.

## 2.4. Study Route

We performed on-road measurements of air pollutants (BC, PM<sub>2.5</sub>, and UFPs) in four parts of Bengaluru.

The mobile-monitoring route included a central business district (CBD), a residential urban neighbourhood (Malleshwaram, MAL) in north-western Bengaluru, a peri-urban neighbourhood (Kannuru, KAN), and an urban-rural transect (URT, a major road), comprising a total of nearly 150 unique kilometres (which translates to ~5,000 30-m road segments).

KAN is a peri-urban location used by Bruhat Bengaluru Mahanagara Palike (BBMP) for land filling. It is approximately 18 km from CBD and characterised by less traffic (compared with the main city). The area also has a quarry, due to which heavy-duty trucks ply here. The CBD includes MG Road and major roads around Cubbon Park and Vidhan Soudha. The study route reflects variations in the traffic volume, traffic density, driving speeds, and street configurations. The study route is shown in figure 6 on an Open Street Map (OSM) background.

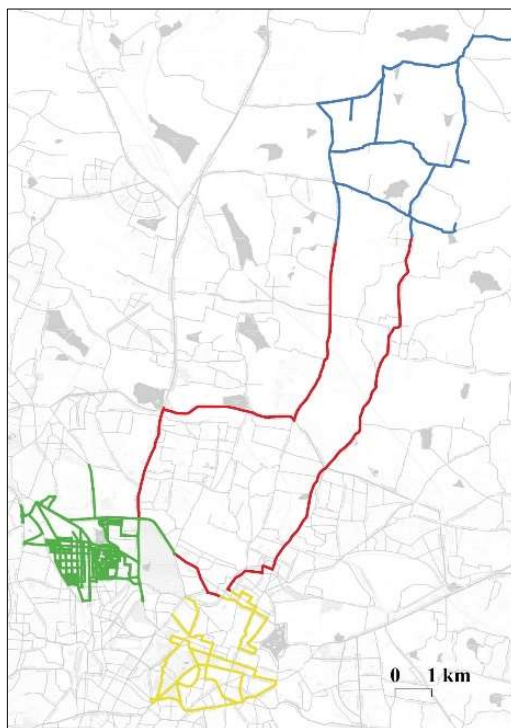


Figure 6 Study route; MAL (green), CBD (yellow), KAN (blue), urban-rural transect (red). The OSM background grey lines indicate roads, while grey patches indicate water bodies and green areas

## 2.5. Study Period

The monitoring campaign started in the month of May 2019 and continued up to the first week of March 2020. There were around 110 measurement days covering all seasons. The measurement days were fewer in the months of December 2019 and January 2020 (6 days in each month) due to unforeseen situations. In August 2019, only nine measurement days were possible because of the rainy and highly humid conditions. On an average, the monitoring days were around 12 per month. All the measurements were carried out on weekdays between 9 am and 1 pm local time, by dividing the entire study route into four parts. The ride on each measurement day covered one part of the study route (which was 30–60 km of road length). Typically, the study route was covered once in a one-week period. In the entire project, the study route was surveyed about 27 times (~6,000 km of driving).





## 3. Results

### 3.1. Number of Measurement Points

In the study period, about 0.95 million 1-second measurements of each of the pollutants ( $PM_{2.5}$ , BC, UFPs) were made. Figure 7 shows the gridded spatial distribution of the number of measurements made during the study period. Clearly, more measurements per road segment were made over MAL, followed by CBD, KAN, and URT. This heterogeneity depended mostly on the speed of the vehicle. In MAL, because of the residential nature and narrow layout of the roads, the monitoring vehicle mostly maintained a speed of 20–30 kmph (kilometres per hour) and collected a relatively greater number of data points per road segment. Over URT and KAN, the typical speed of the vehicle was 50–55 kmph (collecting fewer data points per road segment), unless the vehicle encountered a traffic jam or slow-moving traffic. The median number of measurements per road segment is 116–125 for various pollutants. Apart from the traffic/neighbourhood nature, other factors like road turnings, dead ends, and traffic signals influenced the number of data points collected, owing to the longer manoeuvring time in these areas. For example, there were nearly 76 road segments with more than 1,000 ( $PM_{2.5}$ ) measurements. The number of 1-second BC and UFP measurements were around 5% and 10% less than  $PM_{2.5}$  measurements respectively, because of the data-cleaning procedure and/or instrument malfunction. It has to be noted that the average spatial plots of the pollutants are not marked by aggregating a similar number of measurements over each road segment.

### 3.2. Choice of Central Tendencies

Before preparing the gridded spatial plots of air pollutants, we performed a sensitivity analysis on their central tendencies. In general, air-pollution measurements follow log-normal (i.e., skewed) distribution; a median / geometric mean is a preferred metric to represent their distribution. Aggregates based on the medians and arithmetic means were computed and their relationship investigated. Based on 1-second measurements, we computed daily grid-wise mean and median values for all measurement days. From the daily maps, study-period maps were computed, again using median and mean functions. Study-period average metrics for all the pollutants from daily gridded median and mean values (Median-of-Means; Mean-of-Means; Mean-of-Medians; Median-of-Medians) were computed. A comparison among these metrics for UFPs is shown in the Appendix. All of these metrics followed each other linearly with R-square values greater than 0.95 in all the cases. Mean-of-Medians and Mean-of-Means were slightly higher than other two metrics. Finally, in the present study, the Median-of-Means metric was used (following Apte et al., (2017)), to represent the study-period average value of the pollutants in each grid.

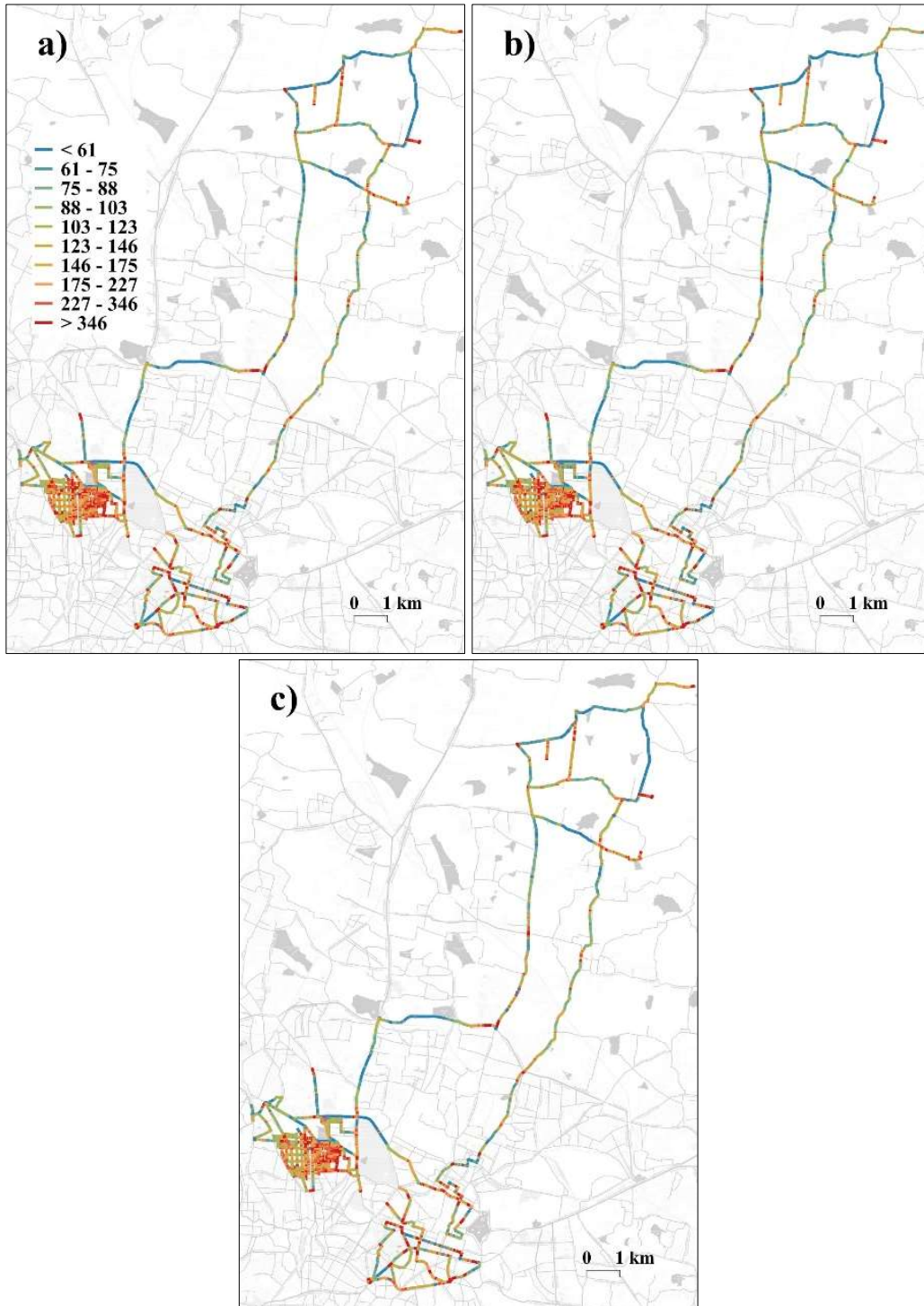


Figure 7 Number of (1-second) measurements made in each 30-m road segment within the study period for a) PM<sub>2.5</sub>, b) BC, and c) UFPs

### 3.3. Spatial Variations

Figure 8 shows the spatial variations in  $PM_{2.5}$ , BC, and UFPs. As discussed above, Median-of-Means is used to plot the study-period spatial-average maps. A zoomed-in plot for MAL is shown in figure 9. A quantile colour-break method is used for the colour ramp. We observed large spatial variability within the study route for all the pollutants. Clearly, the urban residential neighbourhood (MAL) was characterised by lower levels of on-road pollution.  $PM_{2.5}$  (a criteria pollutant) recorded the lowest values (within the study route) over MAL, with a neighbourhood average of around  $28 \pm 4 \mu\text{g m}^{-3}$  (mean  $\pm$  standard deviation (SD)). These values are much below the Indian National Ambient Air Quality Standards (NAAQS) for both daily ( $60 \mu\text{g m}^{-3}$ ) and annual ( $40 \mu\text{g m}^{-3}$ ) averages. Still, the values are much higher than the World Health Organization (WHO) annual standard ( $10 \mu\text{g m}^{-3}$ ). From figure 9, it can be observed that within the residential neighbourhood, there is again a gradient in the pollution levels. The arterials (roads connecting the residential neighbourhood to the major roads) were the next class of roads characterised by relatively higher  $PM_{2.5}$  levels ( $\sim 36 \pm 10 \mu\text{g m}^{-3}$ ). Major roads (highways / Outer Ring Road) displayed the highest levels of pollution ( $PM_{2.5}$ :  $\sim 43 \pm 11 \mu\text{g m}^{-3}$ ). These levels are higher than the annual NAAQS for  $PM_{2.5}$ . The road classifications were based on OSM road features. The road classification map for the study region is shown in the Appendix.

BC and UFPs had a similar pattern, with the lowest values observed over residential neighbourhoods (urban and peri-urban), followed by arterials and major roads. BC values over residential roads, arterials, and major roads were about  $12.8 \pm 5.4 \mu\text{g m}^{-3}$ ,  $25.8 \pm 17.2 \mu\text{g m}^{-3}$ , and  $57.1 \pm 34.3 \mu\text{g m}^{-3}$  respectively. UFPs over residential roads, arterials, and major roads were about  $41,400 \pm 20,000 \text{ cm}^{-3}$ ,  $64,800 \pm 45,500 \text{ cm}^{-3}$ , and  $1,11,500 \pm 55,300 \text{ cm}^{-3}$  respectively.

Next, the coefficient of variation (CV) of the pollutants' distributions were calculated to compare their spatial variability. The results revealed that for all road types, BC and UFPs showed larger spatial variability than  $PM_{2.5}$  did. In addition, one-way analysis of variances (ANOVA) and pairwise t-tests indicated that the differences observed in the pollutant concentrations across the various road types were statistically significant. These values are listed in Table 1, and the box plots are shown in Figure 10. Median and inter-quartile ranges (IQR) are also given in Table 1.

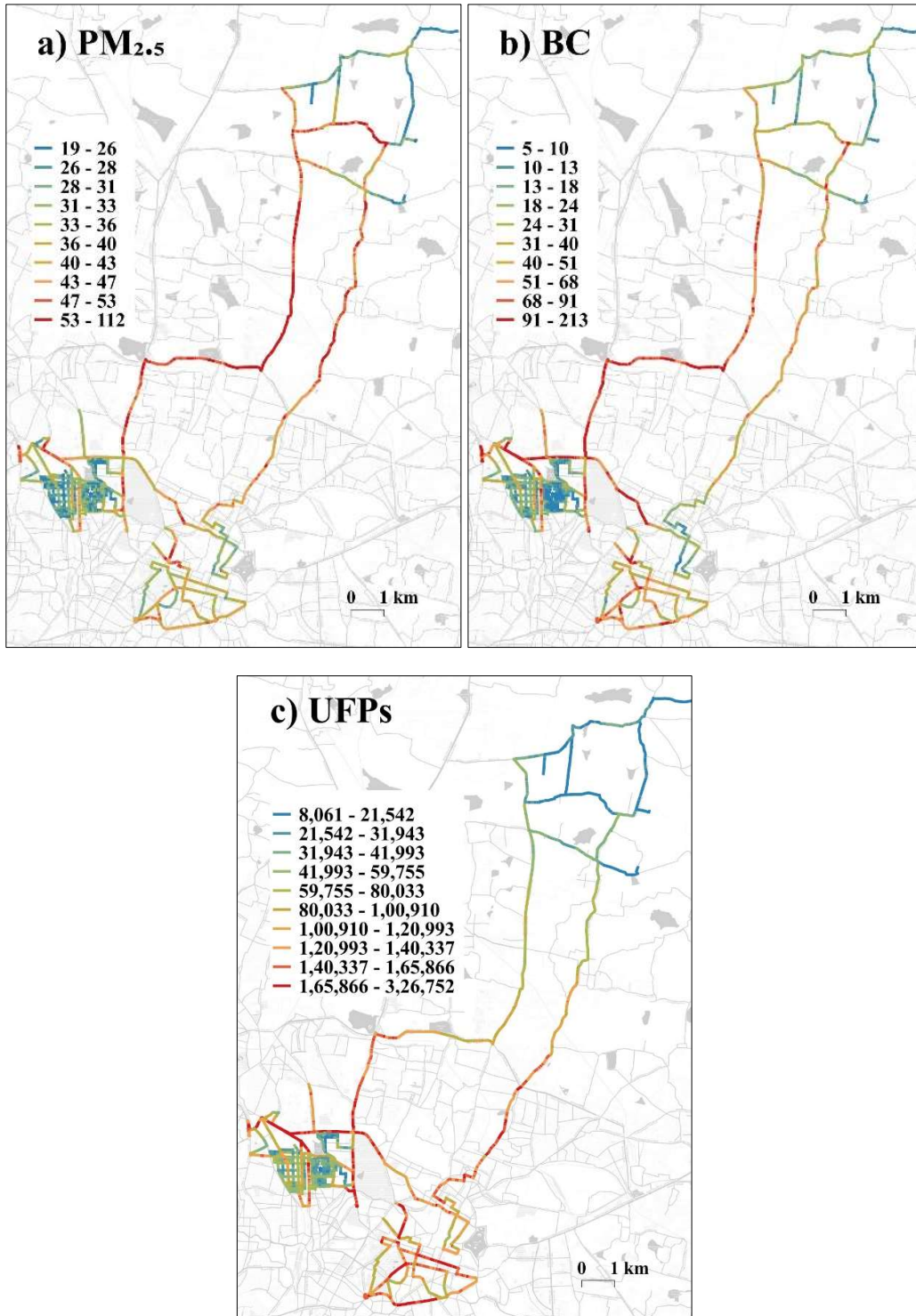


Figure 8 Spatial maps of various pollutants



Figure 9 Zoomed-in spatial maps for MAL

Table 1 Pollutant statistics as per road classification

Pollutant/Metric	Mean	SD	CV (%)	Median	IQR
<b>Major roads</b>					
PM <sub>2.5</sub> (µg m <sup>-3</sup> )	43	11	26	42	14
BC (µg m <sup>-3</sup> )	57.1	34.3	60	49.4	47.9
UFPs (cm <sup>-3</sup> )	111,500	55,300	50	116,300	80,900
<b>Arterials</b>					
PM <sub>2.5</sub> (µg m <sup>-3</sup> )	36	10	28	33	9
BC (µg m <sup>-3</sup> )	25.8	17.2	67	21.6	16.8
UFPs (cm <sup>-3</sup> )	64,800	45,500	70	61,600	74,600
<b>Residential roads</b>					
PM <sub>2.5</sub> (µg m <sup>-3</sup> )	28	4	14	28	5
BC (µg m <sup>-3</sup> )	12.8	5.4	42	11.6	5.9
UFPs (cm <sup>-3</sup> )	41,400	20,000	48	36,000	20,300

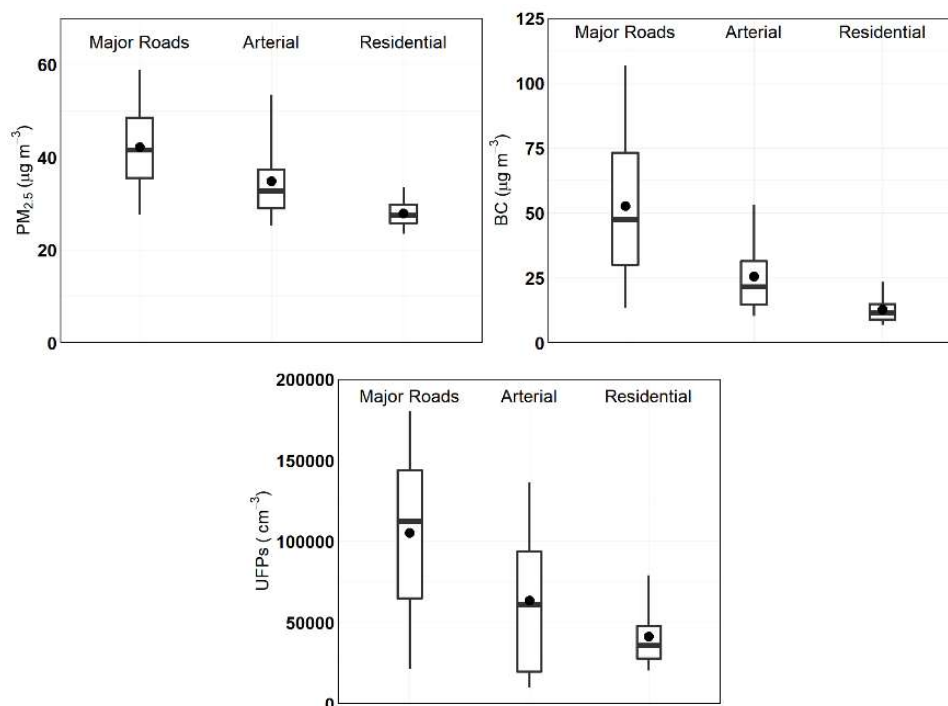


Figure 10 Distribution of pollutants as per road classification. A steeper gradient is seen in BC compared with the others. In the box plot, the solid dot represents the mean, central line of the box represents the median, and the box represent the 25 and 75 percentiles, whiskers represent the 5 and 95 percentile values of the distribution

### 3.4. Stability Analysis

We performed a Monte-Carlo sub-sampling analysis (as detailed in Apte et al., 2017) to understand the representativeness of the spatial pattern of pollutants derived from the mobile-monitoring data and to investigate whether a short-term campaign can reliably reproduce the long-term observed spatial pattern (derived using the full data obtained during the campaign). The spatial pattern derived from randomly sub-sampled unique day's data was compared with the long-term pattern, and R-square values were computed. Conceptually, the R-square value converges to one, as the sub-sample size increases and equals to the total measurement days of the campaign (~27 repeat measurements). A total of 100 draws (100 sub-sampled maps) were made at each N (unique number of measurement days;  $N = 3, 6, 9, 12, 15, 18, 21, 24$ ), and 100 R-square values were derived. The results are shown in Figure 11; surprisingly, a point of 'diminishing returns'<sup>1</sup> is hard to identify from the figure. A closer look reveals that at least 10 repeat measurements<sup>2</sup> are required to make a stable and representative spatial map of pollutants.

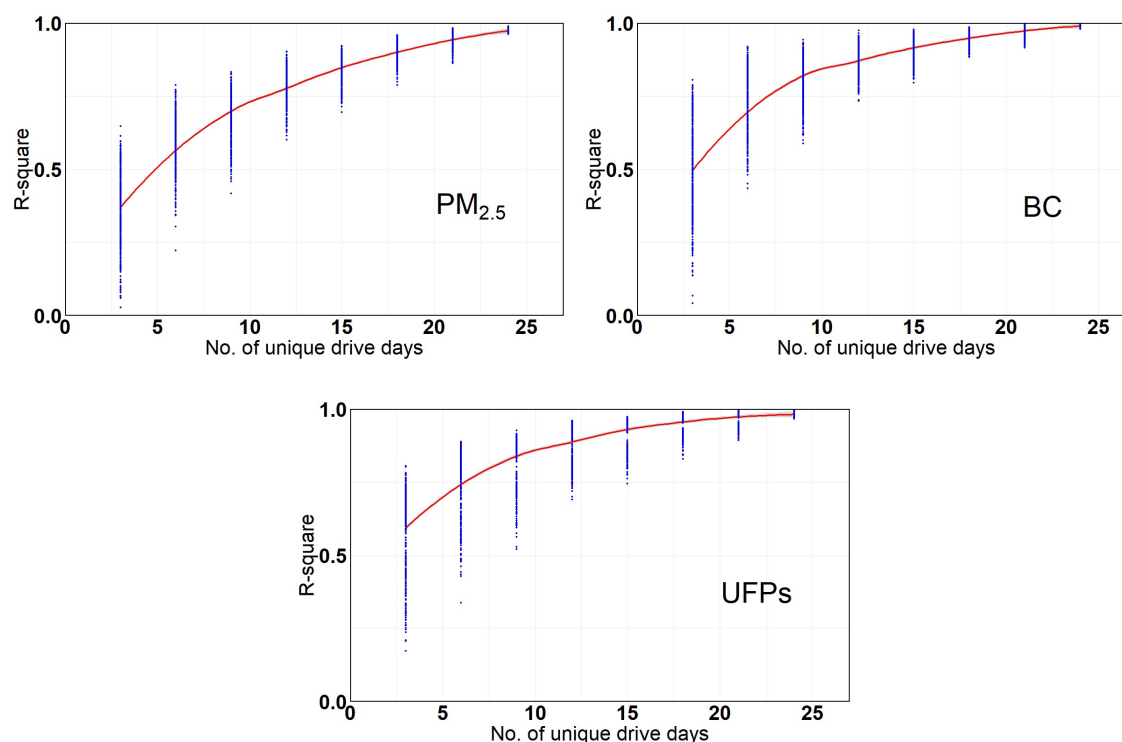


Figure 11 Monte-Carlo sub-sampling analysis for PM<sub>2.5</sub>, BC and UFPs

<sup>1</sup>a point beyond which little improvement is observed in the spatial pattern with additional repeat measurements

<sup>2</sup> beyond which the R-square curve tends to saturate

### 3.5. Comparison with Ambient Data

This step involved the comparison of mobile-monitoring data of on-road PM<sub>2.5</sub> and BC with ambient measurements made at CSTEP and also with various Karnataka State and Central Pollution Control Board’s (KSPCB’s and CPCB’s) data measured across various parts of the city. PM<sub>2.5</sub> measurements at CSTEP and KSPCB/CPCB locations were made using reference-grade instrumentation. BC was compared only with that of CSTEP ambient measurements. No ambient UFP measurements were available. Figure 12 shows the month-wise distribution of the on-road and ambient PM<sub>2.5</sub>.

On-road PM<sub>2.5</sub> values were higher than the ambient PM<sub>2.5</sub> values. On-road PM<sub>2.5</sub> distribution was highly skewed, with a long tail towards the higher values. Summary statistics are given in Table 2. On an average, the on-road PM<sub>2.5</sub> was around 1.6 times the ambient PM<sub>2.5</sub> (combining all ambient stations). Moreover, in August and October, the on-road PM<sub>2.5</sub> values were more than twice the ambient PM<sub>2.5</sub> values.

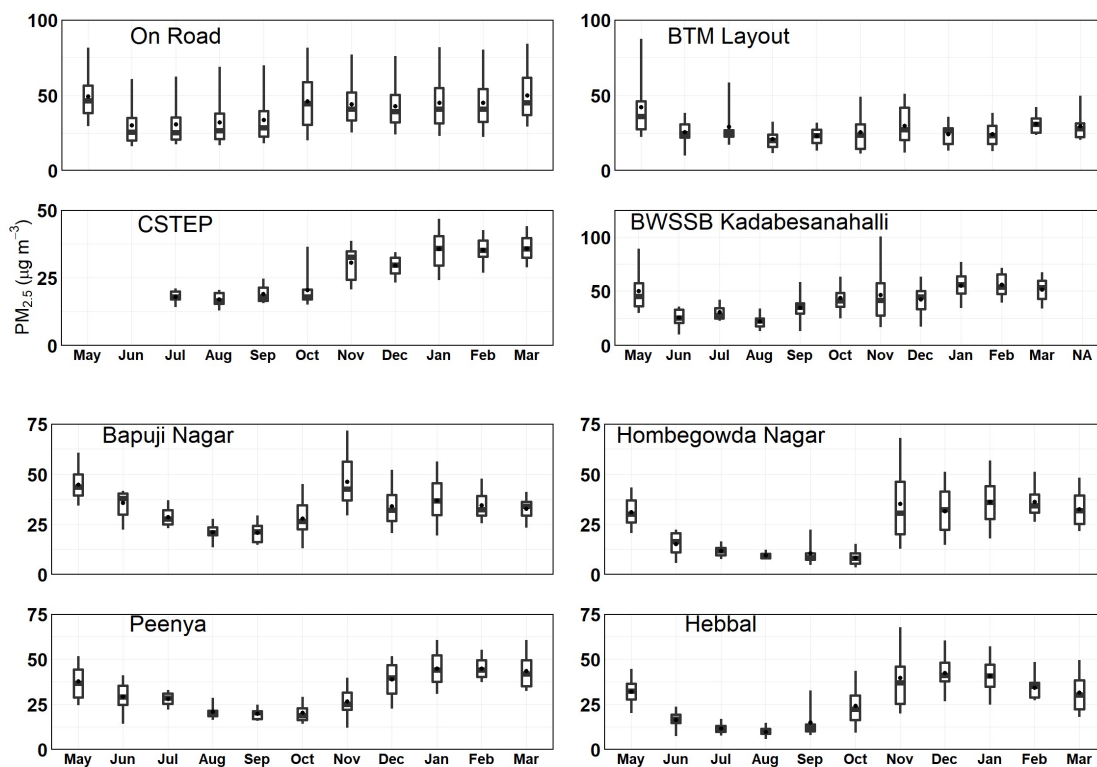


Figure 12 Comparison of (1-second) on-road and ambient PM<sub>2.5</sub>. In the box-plot, solid dot represents the mean, central line of the box represents the median, and the box represent the 25 and 75 percentiles, whiskers represent the 5 and 95 percentile values of the distribution



Table 2 Monthly mean on-road and ambient PM<sub>2.5</sub> (from various measurement sites, in µg m<sup>-3</sup>)

Month	On-road	CSTEP	Bapuji Nagar	Peenya	BTM Layout	BWSSB Kadabes anahalli	Hombe gowda Nagar	Hebbal
May 2019	58	No data	45	38	44	50	31	32
June 2019	32	No data	36	29	25	26	15	16
July 2019	34	18	29	28	29	31	12	12
August 2019	36	17	21	21	21	22	10	10
September 2019	39	19	21	20	23	35	11	15
October 2019	52	20	28	20	25	44	08	24
November 2019	51	31	46	26	47	49	35	40
December 2019	47	29	34	39	27	42	32	42
January 2020	53	36	37	45	24	55	36	42
February 2020	53	35	34	45	31	59	36	34
March 2020	60	36	32	43	29	51	33	23

The absolute values and the spatial variability of the on-road BC are higher than the on-road PM<sub>2.5</sub>. No seasonality was observed in the on-road BC values. A comparison between on-road and ambient BC is shown in figure 13 and table 3. On an average, BC is around 11 times higher (during October, 14 times higher) on-road than in the ambient.

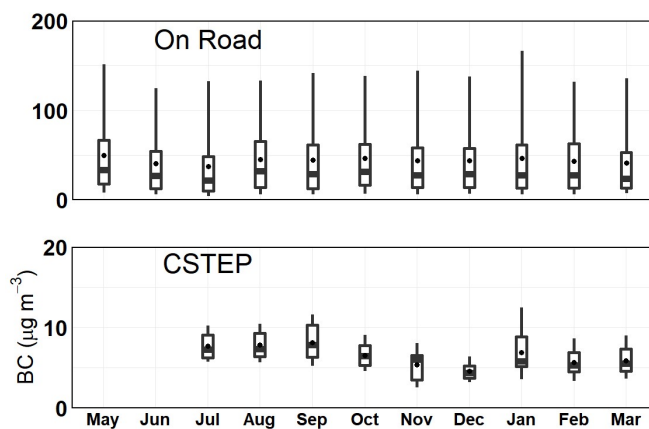


Figure 13 Comparison of on-road and (CSTEP) ambient BC.

Table 3 Monthly mean on-road and ambient BC (in  $\mu\text{g m}^{-3}$ )

Month	On-road	CSTEP
May 2019	68.9	No data
June 2019	53.2	No data
July 2019	58.6	7.7
August 2019	65.5	7.8
September 2019	73.7	8.1
October 2019	93.8	6.5
November 2019	70.3	5.4
December 2019	57.9	4.5
January 2020	65.4	6.9
February 2020	61.1	5.7
March 2020	70.7	5.8

### 3.6. Spatial Gradient and Hotspot Areas

The spatial patterns clearly illustrated the large spatial variability in the pollutant concentrations. As discussed earlier, the SD, IQR, and CV values revealed that the spatial variability of BC and UFPs was larger than that of  $\text{PM}_{2.5}$ . To better understand the spatial gradients, the pollutant concentrations were plotted against the distance from the city centre. As the CBD lies in the central part of the city, it was chosen as the origin and aerial distances were calculated for each 30-m road segment from CBD. Figure 14 shows the variation in the pollutant concentrations on moving away from the city centre.

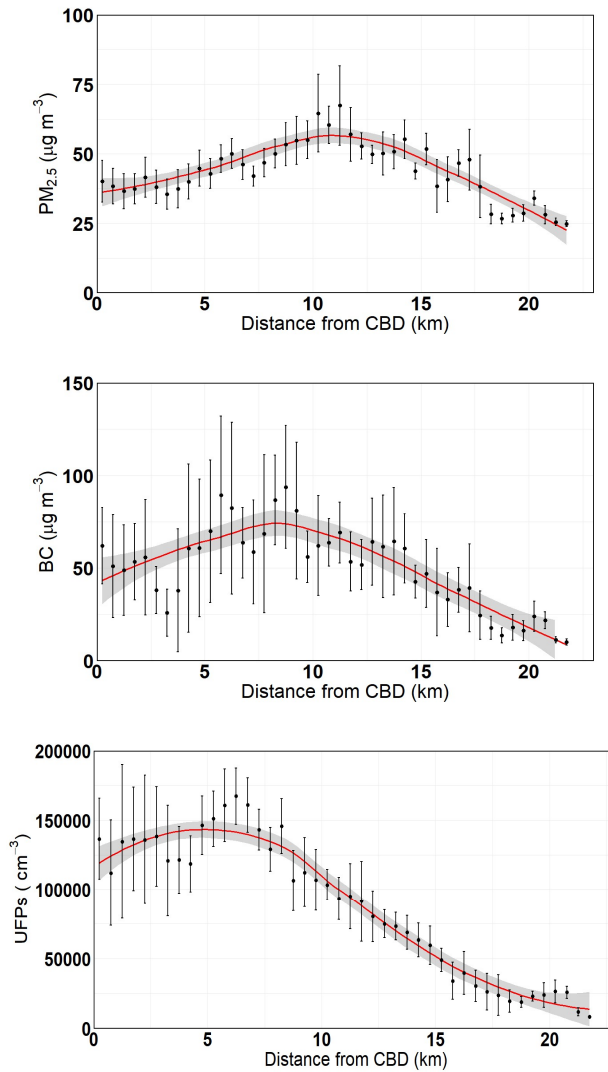


Figure 14 Spatial gradients in PM<sub>2.5</sub>, BC and UFPs. The red line represents the fitter polynomial, and the shaded part represents the 95% confidence interval (CI). Only the major roads were considered to plot the gradients.

Clearly, the city centre is not a pollution hotspot in the case of Bengaluru. In addition to some of the busiest commercial areas, the CBD encompasses large green spaces (e.g., Cubbon Park). Also, the hotspot areas are not the same for all pollutants. PM<sub>2.5</sub> peaks (reaching ~60 µg m<sup>-3</sup>) 10–12 km from the city centre, while BC peaks (reaching ~75 µg m<sup>-3</sup>) 7–9 km away from the city centre. A clear peak was not seen in UFPs, but values remained high (reaching ~1,50,000 cm<sup>-3</sup>) till 7 km away from the city centre.



## 4. Conclusions and Way forward

The present study involved an 11-month-long mobile monitoring of various particulate air pollutants ( $PM_{2.5}$ , BC, UFPs) over a fixed 150-km road stretch, comprising major, arterial, and residential roads in Bengaluru. This is one of the first large-scale (comprising over a million datapoints) mobile-monitoring studies in India. The research team completed a total of 27 repeat measurements over the study route to construct a long-term mean pollution map. The study route was divided into four parts, and each part was covered in one measurement day—which spanned almost four hours, from about 9 am to 1 pm (capturing the rush-hour peak). We followed best practices (relating to instrument calibration, inter-comparison of data from similar instruments, collocation with fixed site measurements, etc.) for a mobile-monitoring campaign of air pollutants, as listed by Alas et al. (2019).

We observed a large spatial variability along the study route for all pollutant concentrations. Urban and peri-urban residential neighbourhoods recorded the lowest  $PM_{2.5}$ , BC, and UFP concentrations, whereas major roads recorded the highest concentrations. Within the neighbourhoods, concentrations varied with the road type. BC, and UFPs displayed larger spatial variability than  $PM_{2.5}$ . Additionally, each pollutant peaked in different regions along the study route. For accuracy, we oversampled the study route (27 repeat measurements); only 10 repeat measurements are required to construct stable high-resolution maps. Irrespective of the road classification and season, on-road  $PM_{2.5}$  levels were higher than ambient. A shallow monsoon trough was observed in  $PM_{2.5}$  (which is not seen in the other pollutants).

The measured on-road concentrations for major roads were higher for BC than for  $PM_{2.5}$ ; that outcome, for actual concentrations, *is nearly impossible (BC is one component of  $PM_{2.5}$  and nearly all BC is smaller than 2.5 microns in diameter, so unless there is a measurement error, any real concentration of BC generally cannot be greater than  $PM_{2.5}$ )*. This outcome in the measurements could be due to monitoring artefacts. First, BAM calibration factor was derived from ambient measurements; it was applied here to in-vehicle measurements. Second, the loading-correction equation used in this study was derived for freshly emitted diesel exhaust. In Bengaluru, garbage/waste burning also contributes to the observed on-road BC, in addition to the diesel emissions.

Air-quality monitoring forms a critical component of various stages of air-quality management. India has nearly  $PM_{2.5}$  200 monitoring stations (operational during 2010-2016), which translate to just about 1 monitor per 6.8 million people (Brauer et al., 2019). However, the country needs about 4,000<sup>3</sup> stationary monitors (2,800 in urban and 1,200 in rural areas) to capture the spatial and temporal variability of air quality. While India is steadily expanding its ground-based monitoring network, high cost remains an impediment. Mobile monitoring is one of the few approaches available to capture concentrations at a high resolution (<100 m). A recently developed framework for India discusses the possibility of using an integrated approach with periodic use of mobile platforms to capture high-resolution spatial and temporal data (Brauer et al., 2019). The current study demonstrated the feasibility of conducting a mid-cost mobile-monitoring study in low- and middle-income countries.

---

<sup>3</sup> <https://urbanemissions.info/india-air-quality/india-ambient-monitoring-data/>

That said, mobile monitoring could be appropriately customised to study specific sources or regions and zoom in to identify hotspots to be prioritised for policy interventions. By partnering with city transport departments or commercial taxi providers, sensors can be mounted on existing fleets—resulting in more efficient data collection. In the Delhi-NCR region, for instance, the cab-aggregator company Ola, in partnership with Microsoft, is mounting low-cost PM<sub>2.5</sub> sensors on its cars to measure real-time air pollution on the streets. Coupling low-cost sensors with such large fleets increases the spatio-temporal coverage and can inform scientists and policymakers on relative concentration values, pollution trends, and hotspots for further action. In this context, regulatory authorities can also adopt mobile-monitoring exercises to generate spatial air-pollution data, which complements data from stationary monitors in understanding the hyper-local nature of the pollution levels and to identify pollution hotspots.

Going forward, mobile-monitoring studies, which give real-time perspective on spatio-temporal variability, can form a critical component of decision-making on air pollution. Given the advancement in measurement technologies, availability of miniaturised and battery-operated devices may help realise such studies in a low-cost and less-complex manner. The current study is a fitting example of the feasibility of all-season mobile monitoring of air pollution in Indian cities. Developing countries such as India, with heterogenous sources within a locality, provide a fertile ground for studies of this nature.

## 5. References

- Alas, H. D. C., Weinhold, K., Costabile, F., Di Ianni, A., Müller, T., Pfeifer, S., ... & Wiedensohler, A. (2019). Methodology for high-quality mobile measurement with focus on black carbon and particle mass concentrations. *Atmospheric Measurement Techniques*, *12*(9), 4697-4712.
- Apte, J. S., Kirchstetter, T. W., Reich, A. H., Deshpande, S. J., Kaushik, G., Chel, A., ... & Nazaroff, W. W. (2011). Concentrations of fine, ultrafine, and black carbon particles in auto-rickshaws in New Delhi, India. *Atmospheric Environment*, *45*(26), 4470-4480.
- Apte, J. S., Messier, K. P., Gani, S., Brauer, M., Kirchstetter, T. W., Lunden, M. M., ... & Hamburg, S. P. (2017). High-resolution air pollution mapping with Google street view cars: exploiting big data. *Environmental Science & Technology*, *51*(12), 6999-7008.
- Ban-Weiss, G. A., Lunden, M. M., Kirchstetter, T. W., & Harley, R. A. (2009). Measurement of black carbon and particle number emission factors from individual heavy-duty trucks. *Environmental Science & Technology*, *43*(5), 1419-1424.
- Bongaerts, E., Bové, H., Ameloot, M., & Nawrot, T. (2019). Ambient Black Carbon Particles Reach the Fetal Side of Human Placenta. *Environmental Epidemiology*, *3*, 34-35.
- Brauer, M., Guttikunda, S. K., Nishad, K. A., Dey, S., Tripathi, S. N., Weagle, C., & Martin, R. V. (2019). Examination of monitoring approaches for ambient air pollution: A case study for India. *Atmospheric Environment*, *216*, 116940.
- Breathe London Project 2018. Accessed 17th April, 2020. <https://www.breathelondon.org/>.
- Dekoninck, L., Botteldooren, D., Panis, L. I., Hankey, S., Jain, G., Karthik, S., & Marshall, J. (2015). Applicability of a noise-based model to estimate in-traffic exposure to black carbon and particle number concentrations in different cultures. *Environment International*, *74*, 89-98.
- Goel, R., Gani, S., Guttikunda, S. K., Wilson, D., & Tiwari, G. (2015). On-road PM<sub>2.5</sub> pollution exposure in multiple transport microenvironments in Delhi. *Atmospheric Environment*, *123*, 129-138.
- HEI. (2010). Panel on the Health Effects of Traffic-Related Air Pollution. Traffic-Related Air Pollution: A Critical Review of the Literature on Emissions, Exposure, and Health Effects.
- Janssen, N. A., Hoek, G., Simic-Lawson, M., Fischer, P., Van Bree, L., Ten Brink, H., ... & Cassee, F. R. (2011). Black carbon as an additional indicator of the adverse health effects of airborne particles compared with PM<sub>10</sub> and PM<sub>2.5</sub>. *Environmental Health Perspectives*, *119*(12), 1691-1699.
- Kim, K. H., Kabir, E., & Kabir, S. (2015). A review on the human health impact of airborne particulate matter. *Environment International*, *74*, 136-143.
- Kolluru, S. S. R., Patra, A. K., & Sahu, S. P. (2018). A comparison of personal exposure to air pollutants in different travel modes on national highways in India. *Science of the Total Environment*, *619*, 155-164.
- Ohlwein, S., Kappeler, R., Joss, M. K., Künzli, N., & Hoffmann, B. (2019). Health effects of ultrafine particles: a systematic literature review update of epidemiological evidence. *International Journal of Public Health*, *64*(4), 547-559.

Polk, H. S. (2019). State of global air 2019: a special report on global exposure to air pollution and its disease burden. *Health Effects Institute, Boston, MA*.

Schraufnagel, D. E., Balmes, J. R., Cowl, C. T., De Matteis, S., Jung, S. H., Mortimer, K., ... & Thurston, G. D. (2019). Air pollution and noncommunicable diseases: A review by the Forum of International Respiratory Societies' Environmental Committee, Part 2: Air pollution and organ systems. *Chest, 155*(2), 417-426.

Tonne, C. (2017). A call for epidemiology where the air pollution is. *The Lancet Planetary Health, 1*(9), e355-e356.



## 6. Appendix

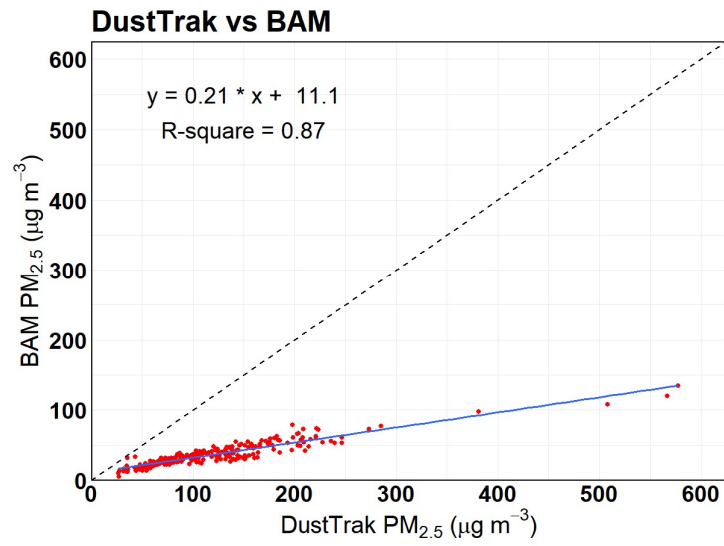


Figure 15 Relationship between DustTrak PM<sub>2.5</sub> and BAM PM<sub>2.5</sub>. Solid blue line indicates the linear least square fit. Dotted line indicates the 1:1 line

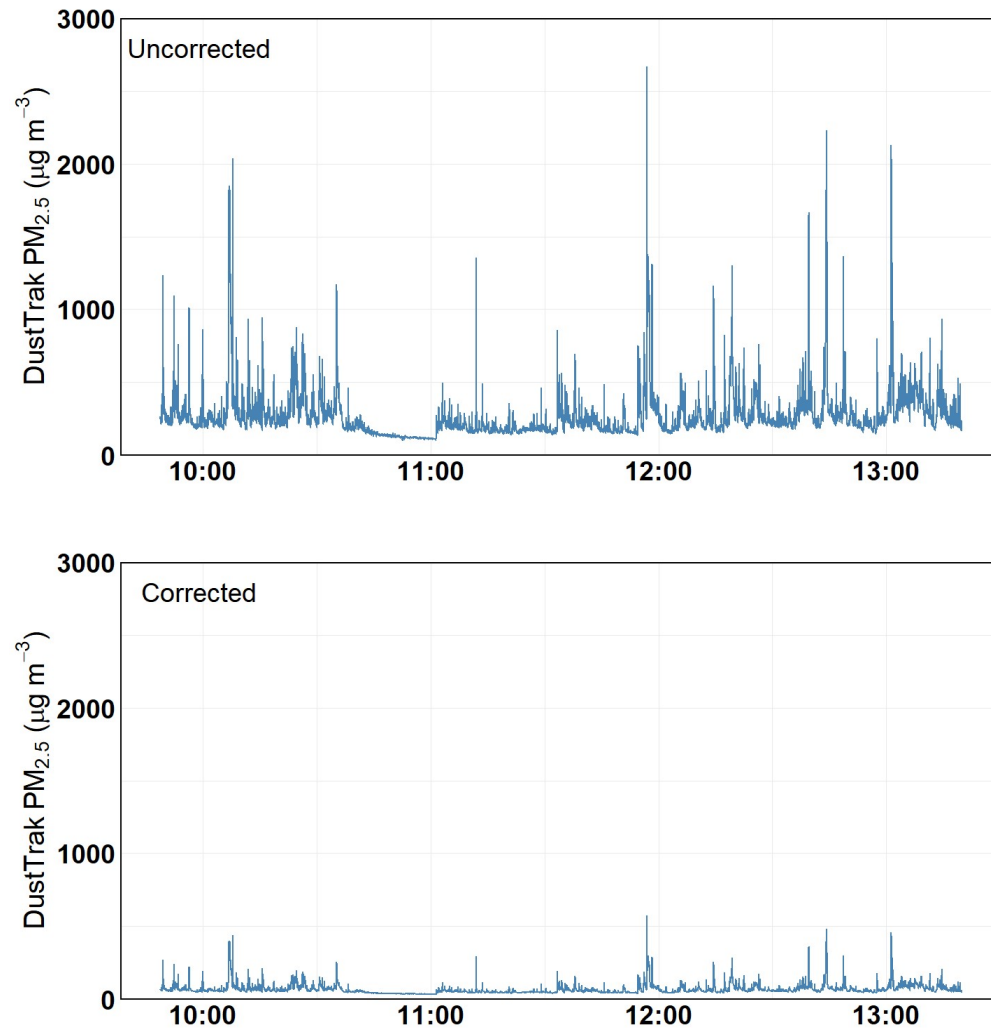


Figure 16 (top panel) Raw PM<sub>2.5</sub> from DustTrak; (bottom panel) BAM corrected DustTrak PM<sub>2.5</sub>

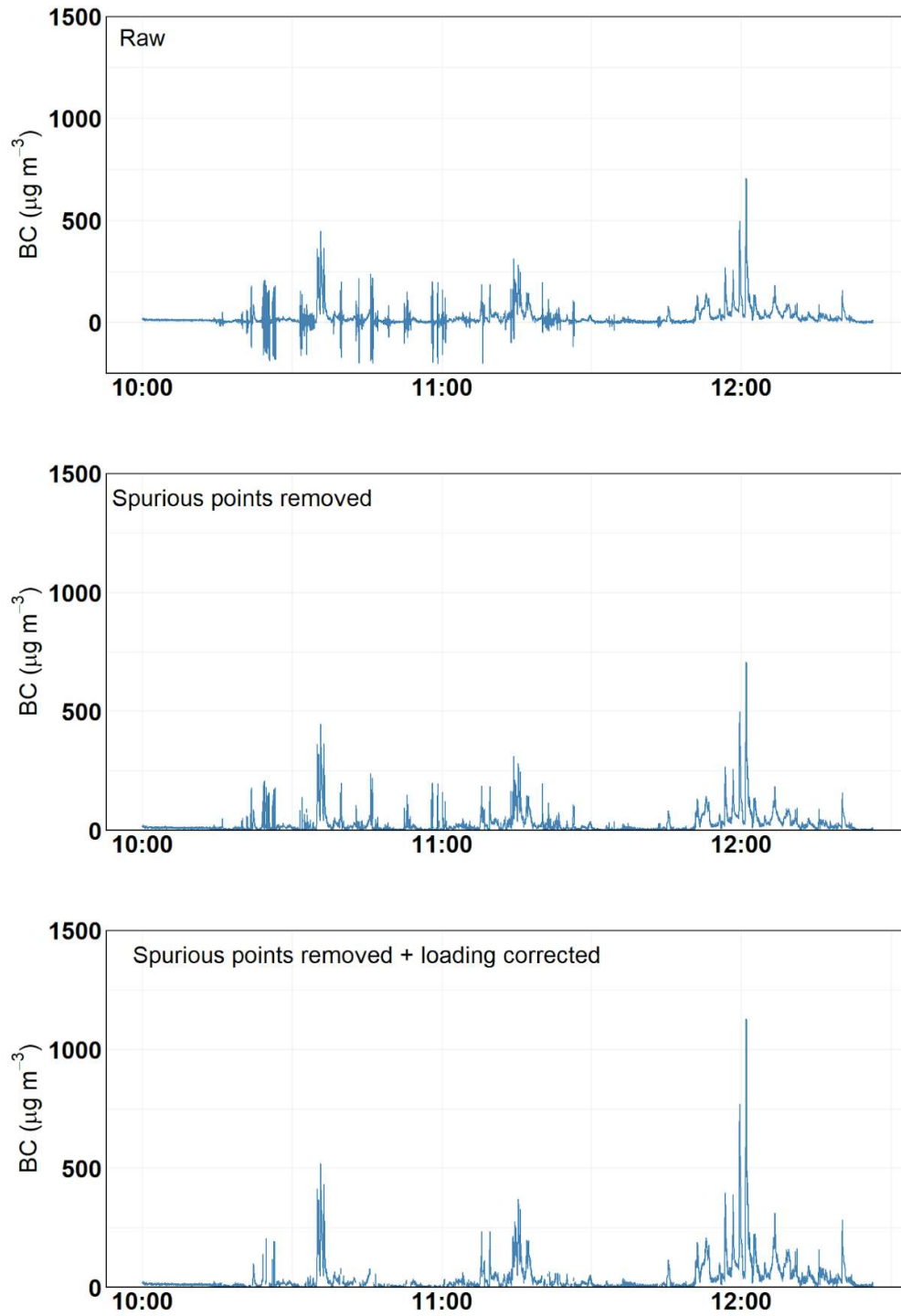


Figure 17 (top panel) Raw BC from AE51; (middle panel) spurious points removed BC; (bottom panel) spurious points removed and loading corrected BC

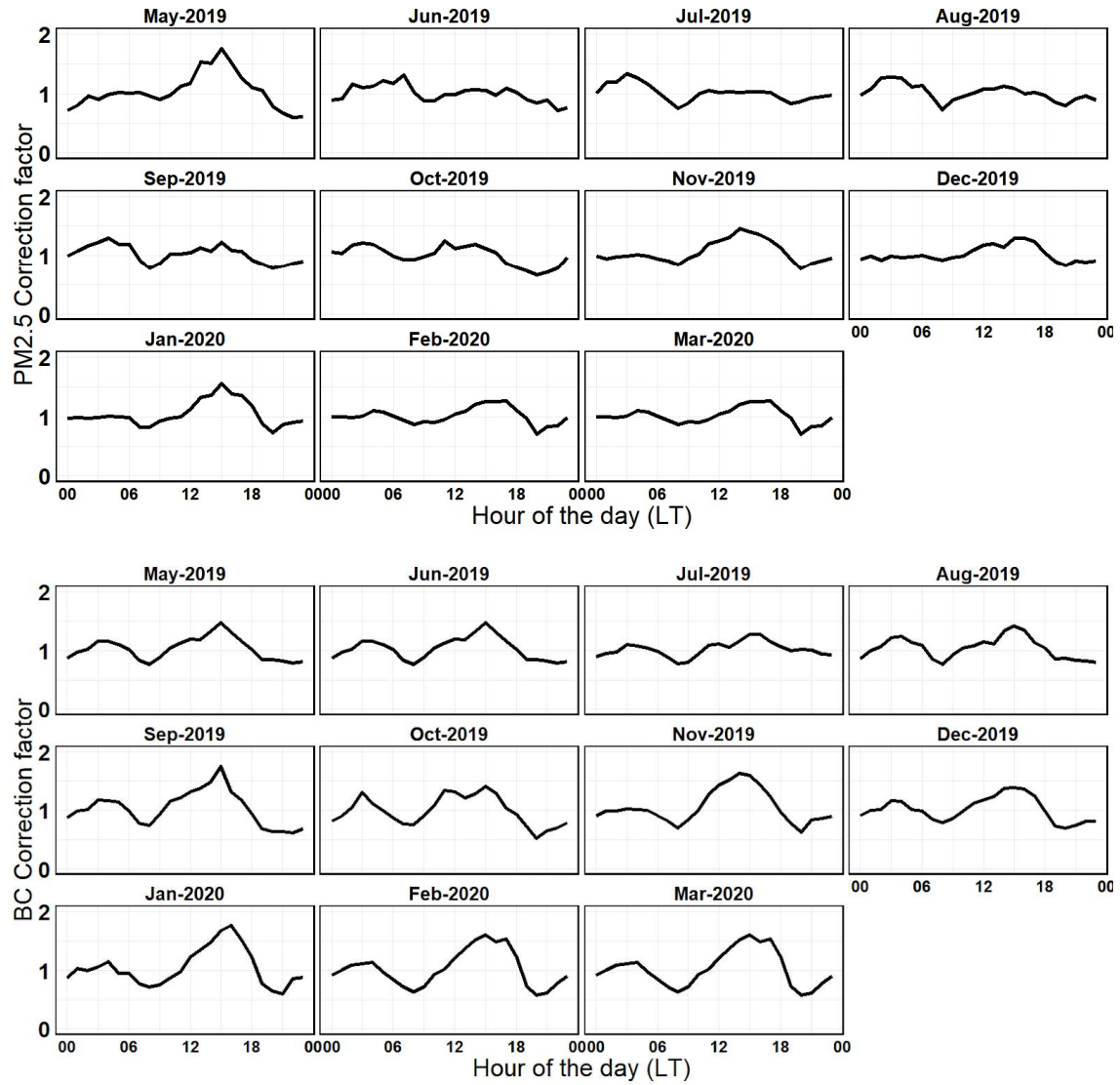


Figure 18 (top panel) Monthly hour-of-the-day correction factors for  $PM_{2.5}$ , and (bottom panel) BC



Figure 19 (top panel) Raw GPS measurements; (middle panel) snapped GPS measurements; (bottom panel) gridded road segments.

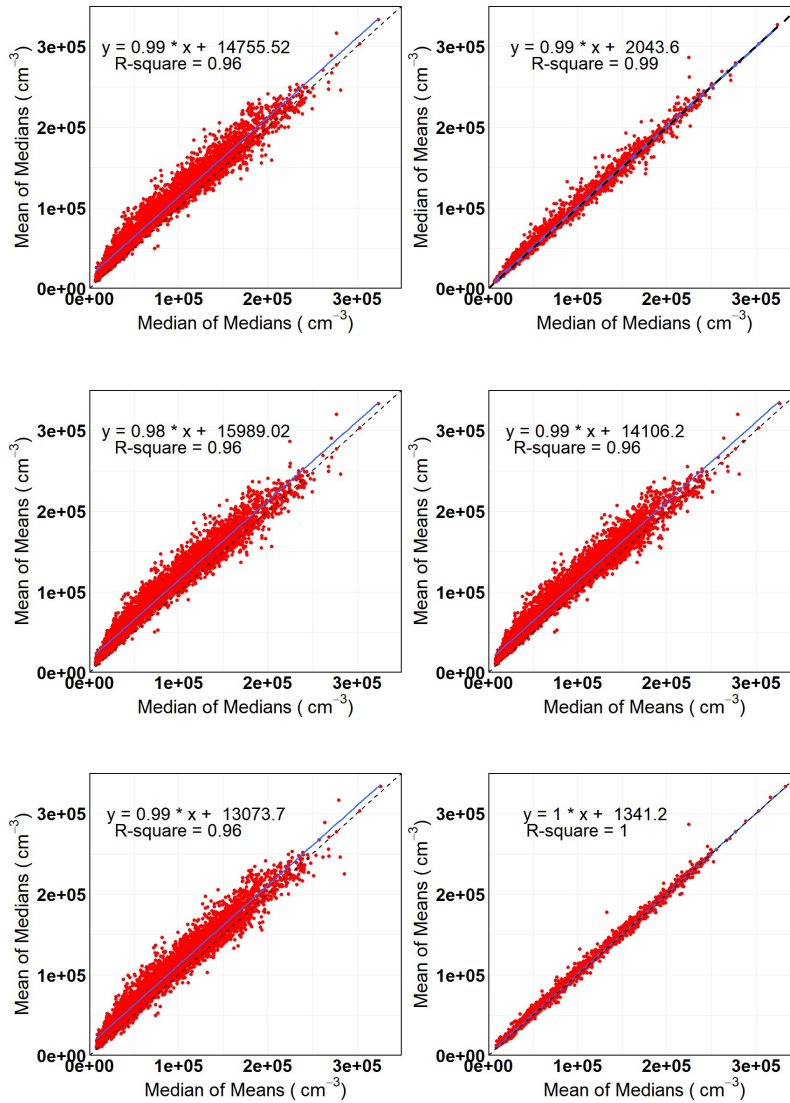


Figure 20 Comparison between various central tendencies (for UFPs). Solid blue line indicates the linear least square fit. Dotted line indicates the 1:1 line. R-square values and the regression coefficients are given in the respective panels

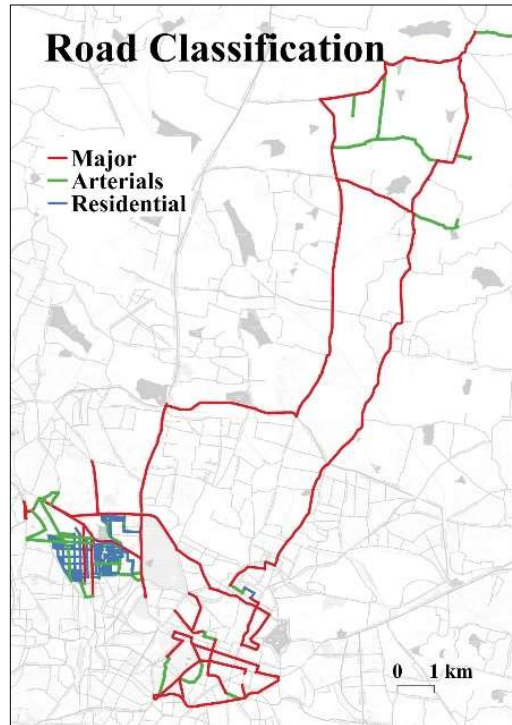


Figure 21 Road classification based on OSM road features. Major roads, arterials, and residential roads consist of 2,895, 1,112 and 983 30-m road segments respectively



## **BENGALURU**

No. 12-14 & 18-19, 10th Cross, Mayura Street,  
Papanna Layout, Nagashettyhalli (RMV II Stage),  
Bengaluru - 560094

## **NOIDA**

1st Floor, Tower-A,  
Smartworks Corporate Park,  
Sector-125, Noida-201 303

E-mail: [cpe@cstep.in](mailto:cpe@cstep.in)

[www.cstep.in](http://www.cstep.in)